Science Journal of University of Zakho
DOI: https://doi.org/10.25271/sjuoz

Original Article

MULTIFUNCTIONAL CARBON QUANTUM DOTS DERIVED FROM GREEN BEAN SEEDS FOR COPPER (II) ION SENSING, NANOTHERMOMETRY, AND ANTIBACTERIAL APPLICATIONS

Aveen Ramadhan Qasim[1, *], and Diyar Sadiq[2]

[1]Department of Physics, College of Science, University of Zakho, Zakho, Kurdistan Region, Iraq.
[2]General Director of the Scientific Research Center, Duhok Polytechnic University, Duhok, 61 Zakho Road, Kurdistan Region, Iraq.

[*]*Correspondence author. E-mail:* aveen.qasim@staff.uoz.edu.krd (Tel: +964-7507498949)

Received: 28, Jun, 2025

Accepted: 17, Aug, 2025

Published: 12, Apr, 2026

ABSTRACT

The increasing global demand for inexpensive and environmentally friendly fluorescent nanomaterials highlights the urgency of employing green synthesis approaches using biomass-based materials. Following the principles of green chemistry, the present study details a one-step hydrothermal synthesis of carbon quantum dots using green bean seeds as a carbon precursor, with no chemical additions. Photoluminescence (PL) spectroscopy showed excitation-dependent fluorescence properties with a peak green emission at 532 nm when excited at 490 nm and a quantum yield of 37.1%. Transmission electron microscopy (TEM) revealed uniform quasi-spherical nanoparticles (~5 nm). X-ray diffraction (XRD) confirmed a graphitic core. Fourier transform infrared spectroscopy (FTIR) and energy-dispersive X-ray spectroscopy (EDX) analyses revealed surface carbonyl and hydroxyl groups, with carbon and oxygen as principal elements. The CQDs demonstrated nanosensing capability for Cu^{2+} ions, with a limit of detection of 0.1 µM via fluorescence quenching. Temperature-dependent PL studies exhibited linearity in the 20 to 65°C range with a relative thermal sensitivity of 1.17% $°C^{-1}$, confirming the nanothermometer capability of CQDs. Using the serial dilution method, CQDs represent antibacterial activity against *Escherichia coli* and *Klebsiella* bacteria. Multifunctional green bean-based CQDs have excellent potential for nanoscale temperature, heavy metal sensing, and biomedical applications.

KEYWORDS: Green Synthesis, Carbon Quantum Dots (CQDs), Green Bean Seeds, Sensor, Antibacterial Activity.

1. INTRODUCTION

Much interest has been directed toward carbon quantum dots (CQDs) over the last decade, as they are a member of a growing class of carbon-based nanomaterials with dimensions less than 10 nm and exhibit outstanding luminescent performance, biocompatibility, and minimal environmental impact. The important optical and physicochemical features of CQDs, such as bright fluorescence, resistance to photobleaching, excitation-dependent emissions, high quantum yields, low toxicity, smaller sizes, enhanced solubility in water, chemical stability, and simplicity of functionalizing, have inspired significant research on their potential uses (Scaria *et al*., 2020; Sciortino *et al*., 2018; Yadav *et al*., 2023). These applications span biomedical fields such as bio-imaging (Das *et al*., 2024), cellular imaging (Xu *et al*., 2021), bio-labelling (Sharma *et al*., 2020), drug delivery (Molaei, 2023), metal sensing (Das *et al*., 2020), energy storage (Kumar *et al*., 2022), optoelectronics (Yuan *et al*., 2019), sensors (Li *et al*., 2021), light-emitting diode (Bucka *et al*., 2024), pH sensing (D'Souza *et al*., 2024), temperature sensing (Hu *et al*., 2022) and antibacterial activity (Gagic *et al*., 2020).

Researchers have developed different synthesis techniques to generate CQDs, which generally fall into two categories: top-down and bottom-up approaches. Many studies have focused on creating straightforward,

Access this article online

https://doi.org/10.25271/sjuoz.2026.14.2.1651

Printed ISSN 2663-628X;
Electronic ISSN 2663-6298

Science Journal of University of Zakho
Vol. 14, No. 02, pp. 267 –279 April-2026

inexpensive, and effective methods for CQD production, emphasizing safety and sustainability. In the top-down approach, scientists break down large carbon structures such as graphite, carbon nanotubes, and graphene oxide into smaller pieces using techniques like arc discharge, laser ablation, and electrochemical methods. In contrast, researchers synthesize CQDs suitable for large-scale production through bottom-up approaches by assembling small organic precursor molecules. This process involves hydrothermal or solvothermal treatments, pyrolysis, microwave irradiation, or combustion (Kong *et al*., 2024; Magesh *et al*., 2022; Yadav *et al*., 2023). The field of hydrothermal green synthesis of CQDs is rapidly expanding. Its low production cost, one-step synthesis, low reaction temperatures and long-term sustainability make this method environmentally friendly and widely accessible, with minimal use of hazardous chemicals (Nazibudin *et al*., 2023; Xie *et al*., 2019).

Precursor selection significantly influences the fluorescent and overall properties of CQDs due to the strong relationship between surface groups and the carbon source composition. Optimizing precursor choice and reaction parameters can enhance the photoluminescence characteristics of CQDs (Chahal *et al*., 2021; Verma *et al*., 2022). Notably, surface functionalization can be achieved naturally, without chemical doping or passivation, due to the abundance of biomolecules such as carbohydrates and proteins present in plant-based precursors. Thus, plants provide unique and effective building blocks for sustainable CQD synthesis (Zulfajri *et al*., 2020). A variety of natural and food-derived materials have been investigated as carbon sources for CQD synthesis, such as fruit peels, juices, chicken eggs, vegetables, and plant leaves (Feng *et al*., 2015; Mehta *et al*., 2015; Yin *et al*., 2013; Zhang *et al*., 2015). Legume-based precursors, such as black soybeans, mung beans, and red lentils, have been studied due to their abundant biochemical composition. The literature indicates that these materials have achieved high quantum yield (QY) values, particularly when enhanced through nitrogen doping (Jia *et al*., 2019; Kaur *et al*., 2019; Khan *et al*., 2019).

However, to the best of our knowledge, green bean seeds have not yet been reported as a precursor for CQD synthesis. Green beans represent an economical and sustainable food source, with a carbohydrate content ranging from approximately 50–68%. They also contain significant amounts of bioactive compounds and functional proteins (Singh *et al*., 2021). This study demonstrates that green bean seeds can yield a high quantum yield without requiring chemical additives, and offer multifunctional capabilities compared to previously investigated legumes. The distinctive biochemical composition of green bean seeds positions them as a promising candidate for the sustainable and efficient production of CQDs. This work presents a straightforward hydrothermal approach using green bean seeds for the low-cost and eco-friendly synthesis of fluorescent CQDs. A range of experimental and spectroscopic techniques was employed to characterize the synthesized CQDs and explore their potential applications in antibacterial activity, nanoscale temperature sensing, and the selective detection of Cu^{2+} ions.

2. MATERIALS AND METHODS

Experimental Materials:

Fresh green beans were purchased from a local market in Zakho, Kurdistan region, Iraq. The beans were hulled to remove the outer layer, then thoroughly washed several times with distilled water to eliminate dirt and contaminants. After washing, the beans were sun-dried for two days to ensure complete moisture removal. The dried green bean seeds were then ground using a mixer until a fine, uniform powder was obtained. This green bean powder was used as a carbon precursor for carbon quantum dot synthesis. Distilled water was produced with the help of a Milli-Q ultrapure water purification system. Lastly, fluorescein dye ($C_{20}H_{12}O_5$, MW: 332.31 g/mol) was obtained from Sigma-Aldrich and used in this study.

Instrumentation and Synthesis Equipment:

A Japanese JEOL JEM 1010 TEM was used for transmission electron microscopy (TEM) analysis. SEM/EDX analysis was conducted on an SEM FEI Quanta 250 FEG, USA. A Bruker D8 Discover X-ray diffractometer (Germany) was used for X-ray diffraction (XRD) analysis. It employed Cu Kα radiation (λ = 0.154060 nm) over a 2θ range of 5° to 80°, at 40 kV and 30 mA. JASCO FTIR/4000 instrument (Japan) was used for Fourier Transform Infrared Spectroscopy (FTIR) analysis. For photoluminescence (PL) analysis, a handmade fluorescence spectrophotometer equipped with a tunable light source and a SCIENCETECH9702 spectrometer (Canada) was utilized. UV–Vis absorption spectra were recorded using a CECIL CE 7200 spectrophotometer. A Magnetic Stirrer and Hot Plate (HS-12, China) were also used during sample preparation. Hydrothermal synthesis was performed in a 100 mL stainless-steel autoclave equipped with a Teflon (PTFE) layer. Centrifugation was carried out using a KT7-900-434 high-speed centrifuge (Kenda, Germany's Heller International Trading Co., Ltd). Finally, a constant-temperature drying oven (Model: WHL/50HZ, FAITHFUL, China) was used during the synthesis process.

Synthesis of CQDs:

Figure 1 illustrates the process for synthesizing CQDs. A single-step hydrothermal technique was employed to synthesize CQDs, using distilled water as the solvent and green bean seeds as the carbon precursor. The process includes the following steps: First, a solution was prepared by mixing 4 grams of green bean powder with 40 milliliters of distilled water and allowing it to mix for one hour. The solution was then transferred into a 100 mL autoclave reactor and heated to 200°C for 12 hours in an oven. After cooling to room temperature, the resulting CQD solution was subjected to two stages of purification. Initially, a 10-minute centrifugation at 10,000 rpm was performed to remove larger particles. The supernatant was then filtered using a 0.22 μm membrane filter to eliminate residual impurities and improve purity. The CQD preparation process was thus completed, and the samples were stored at 4 °C until further investigations could be conducted.

Figure 1: A schematic representation illustrating the single-step hydrothermal technique for preparing CQDs from green bean seeds.

Fluorescence Detection of Cu^{2+} Ions:

Green bean-synthesized CQDs were utilized as the sensing material for detecting copper (II) ions (Cu^{2+}). The experiment began with 3 mL of CQD solution in a quartz cuvette. Then, solutions of metal ions at different concentrations were added and allowed to stand for 3 minutes. The PL spectra of the CQDs were recorded using a 300 W xenon arc lamp, with an excitation wavelength of 490 nm. The impact of different metal ions on the fluorescence intensity of the CQDs was assessed at room temperature. Cu^{2+} ions were found to significantly reduce the fluorescence intensity of the CQDs among the tested metals. 230 mg of copper nitrate trihydrate ($Cu(NO_3)_2 \cdot 3H_2O$) was dissolved in 5 mL of distilled water to create a 0.1902 M stock solution of Cu^{2+} ions to examine the impact of Cu^{2+} ion concentration on CQD fluorescence. Different volumes of the stock solution were added to 3 mL of the CQD solution, the mixture was left to equilibrate for three minutes. Fluorescence intensities for CQD solutions with concentrations of Cu^{2+} ranging from 0.09 to 0.17 µM were measured. A calibration curve was constructed to illustrate the relationship between fluorescence quenching intensity and Cu^{2+} ion concentration. To evaluate the effectiveness of the sensing mechanism, a linear regression analysis was performed to determine the slope, standard deviation, coefficient of determination (R^2), and limit of detection.

Temperature-Dependent Fluorescence Intensity of CQDs:

Research into the potential applications of carbon quantum dot solutions in nanothermometry led to this investigation of their temperature sensitivity. A quartz cuvette was placed on a heating plate, and 3.5 mL of the CQD solution was transferred into it. During the experiment, temperatures ranging from 20 to 65 °C were applied in 5 °C increments. A thermometer was inserted into the mixture to obtain accurate temperature readings. Once thermal equilibrium was reached, photoluminescence measurements were taken at the excitation wavelength of 490 nm. A calibration curve was created to demonstrate the correlation between fluorescence intensity and temperature. This method allowed us to evaluate whether the CQDs' fluorescence intensity varied with temperature by measuring their response across a broad temperature range.

Quantum Yield Measurement of CQDs:

The quantum yield (QY) of CQDs was calculated using the single-point relative technique, as is given in equation (1), and outlined in the previous literature (Saber *et al*., 2024; Salman, 2023). To determine the QY of the CQD solution, fluorescein dye, which has a constant quantum yield of 0.95 (Mohammed & Omer, 2020; Mousa *et al*., 2023), was utilized as a reference standard. To minimize the impact of reabsorption, the concentration adjusted to ensure that the absorbance of both the standard and sample solutions at the excitation wavelength of 490 nm remained below 0.1. Afterward, the integrated fluorescence intensity was determined for the standard and sample fluorescence spectra, recorded at the optimal wavelength over the emission range of 490 to 620 nm range.

$$QY_{CQDs} = QY_{ST}\left(\frac{F_{CQDs}}{F_{ST}}\right)\left(\frac{A_{ST}}{A_{CQDs}}\right)\left(\frac{\eta_{CQDs}}{\eta_{ST}}\right)^2 \quad (1)$$

In this context, QY_{CQDs} refer to the fluorescence quantum yield of the carbon quantum dots (sample), whereas QY_{ST} stands for quantum yield of the reference standard. The integrated fluorescence intensities, measured in arbitrary units (a.u.), correspond to the fluorescence emission spectra of the sample (F_{CQDs}) and the reference standard (F_{ST}). Their refractive indices (η) were both 1.33 as distilled water was used to dilute both the reference standard and the sample. A represents the absorbance at the optimum wavelength, also measured in a.u.

3. RESULTS

Morphological, Structural, Surface, and Elemental Characterization of CQDs:

The morphology of the synthesized CQDs was confirmed using transmission electron microscopy (TEM), which provided significant insights into their morphological characteristics and particle size distribution. Figure 2A shows a predominantly quasi-spherical morphology, characterized by well-dispersed nanoparticles with minimal aggregation. The size distribution of the CQDs was narrow, with an average particle size calculated as d_{avg}= 5.01 nm. Based on the particle size analysis conducted using ImageJ software on the TEM image, the CQDs exhibited a diameter range from 2.35 nm to 9.82 nm, as illustrated in the histogram in Figure 2B. X-ray diffraction (XRD) analysis was used to study the crystallinity and internal structure of CQDs. Figure 2C demonstrates that the synthesized CQDs exhibited a distinctive diffraction peak in their XRD spectrum at 24.8°. The observed peak corresponds to the (002) plane of the graphitic carbon crystalline structure, exhibiting an interplanar spacing (d-spacing) of 0.35 nm, calculated using Bragg's equation (Arul & Sethuraman, 2019; Deme *et al*., 2023). However, some additional peaks did not correspond to CQDs and may originate from residual precursors or contaminants. The crystallite size of CQDs for the (002) plane, calculated using the Debye–Scherrer equation, was approximately 8.48 nm (Deme *et al*., 2023).

To identify the functional groups on the surface of CQDs, Fourier transform infrared spectroscopy was used. Figure 2D displays the FTIR spectrum within the 4000-400 cm^{-1} range. The figure reveals a pronounced broad band between 3327 and 3233 cm^{-1} corresponding to the O–H stretching vibrations, suggesting the presence of hydroxyl groups on the CQD surface. The band observed at 1627 cm^{-1} corresponds to the stretching vibration of carbonyl groups (C=O). The peak at 1381 cm^{-1} is attributed to the asymmetric stretching vibration of C–O–C, indicating the presence of ether or epoxy linkages. A small absorption peak at 2101 cm^{-1} confirms the presence of an alkyne group (C≡C), due to the stretching vibration of carbon–carbon triple bonds. Additionally, the elemental composition of the synthesized CQDs was determined using energy-dispersive X-ray (EDX) analysis. As shown in Figure 2E, the EDX spectrum primarily indicates the presence of carbon (57.32%) and oxygen (32.17%), with a minor amount of potassium (10.51%) also detected.

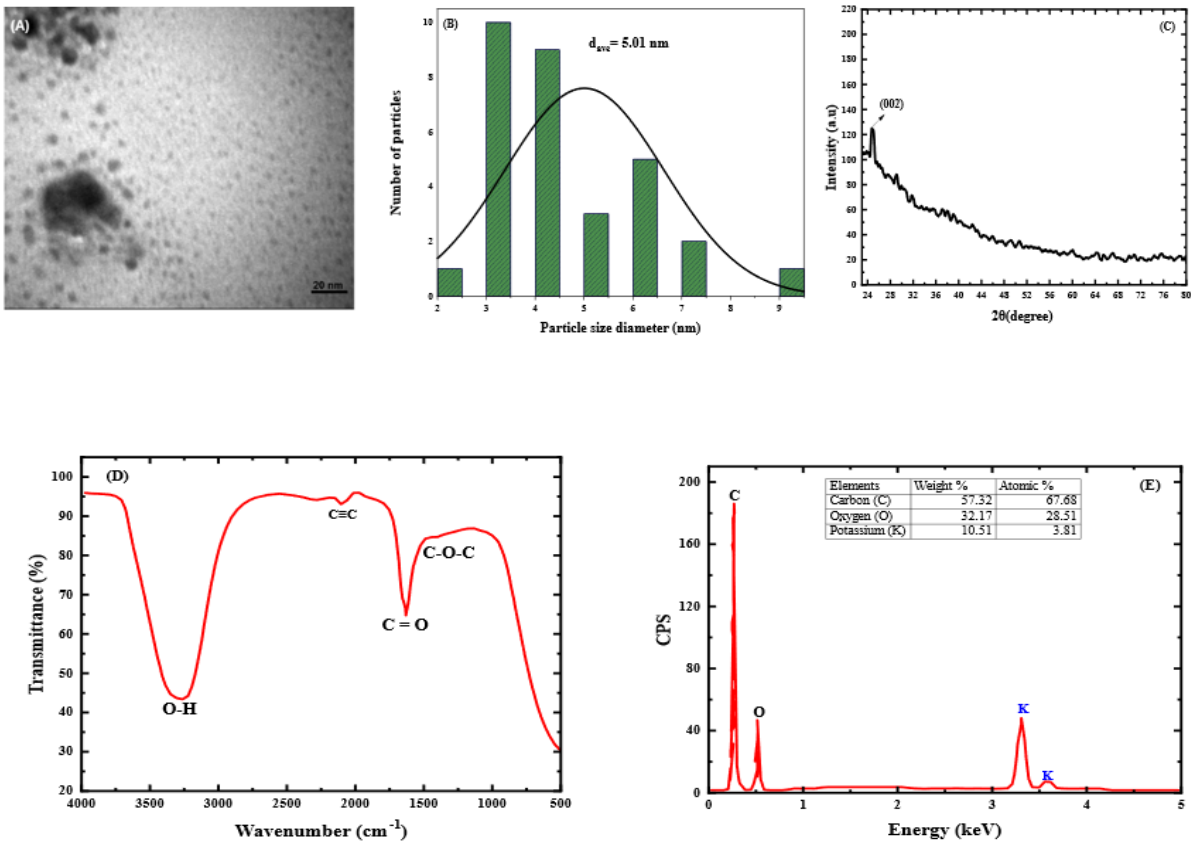

Figure 2: Characterization of the synthesized CQDs: (A) TEM image; (B) Histogram showing the particle size distribution; (C) XRD pattern; (D) FTIR spectrum; (E) EDX spectrum.

Optical Characterization of CQDs:

The optical features of the synthesized CQDs were evaluated by analyzing their fluorescence emission and ultraviolet–visible (UV-Vis) absorption spectra. One of the main properties of CQDs is their tunable photoluminescence, which allows them to emit light across a broad spectrum of wavelengths. Their emission peaks are most noticeable in the ultraviolet, visible, and near-infrared regions. The synthesized CQDs exhibit excitation-dependent emission characteristics, as shown in Figure 3A. The excitation wavelengths used to measure photoluminescence emissions ranged from 430 to 530 nm, with intervals of 10 nm. From 430 to 490 nm, the emission peak becomes increasingly intense with increasing excitation wavelength, accompanied by a redshift of 12 nm, moving from 520 nm to 532 nm. The emission peak reaches its maximum wavelength of 532 nm when excited at 490 nm. Nevertheless, beyond this most pronounced peak, a decrease in photoluminescence intensity is observed as the excitation wavelength increases from 500 nm to 530 nm; a shift toward longer wavelengths is observed in the emission peaks, extending to 556 nm. Also, the fluorescence quantum yield (QY) of the CQDs prepared from green beans was determined to be 37.1%, using fluorescein as the reference standard. Additionally, the aqueous CQD solution exhibited strong green luminescence when exposed to 365 nm ultraviolet light (inset in Figure 3B), confirming that the synthesized CQDs exhibit remarkable photoluminescence characteristics.

Absorption spectroscopy is an extremely efficient approach for investigating the electronic transitions of CQDs. Fluorescent CQD samples were subjected to UV-Vis spectra analysis, recorded between the wavelengths of 200 and 800 nm. In general, pure CQDs exhibit two noticeable absorption peaks. The first one is linked to the π-π* transition of aromatic sp^2 carbons, also known as C=C bonds, corresponding to bands with wavelengths less than 300 nm. The second peak, linked to surface functional groups n–π* transition, arises from intrinsic absorption between 300 and 400 nm (Bandi *et al*., 2016). Figure 3B shows two significant absorption peaks in the synthesized CQDs, with the highest absorption recorded at 274 nm and 317 nm in the ultraviolet region. The absorption maxima at 274 nm and 317 nm for C=C aromatic bonds and functional groups like C=O, respectively, indicate the existence of π-π* and n-π* transitions (Bakier *et al*., 2020; Hu *et al*., 2015). Moreover, the optical characteristics of various materials can be studied by measuring the band gap energy, which is the difference in possible energy between the valence and conduction bands. A Tauc plot was used to determine the optical band gap energy (Eg) using UV-Vis spectral data. It was constructed by plotting $(\alpha h\upsilon)^2$ against hυ, where α is the absorption coefficient, h is the Planck constant, υ is the light frequency, and E is represented as hυ (eV) (Jumardin *et al*., 2021). As indicated in Figure 3C, a careful fit illustrates the indirect transition band gap of CQDs. The synthesized CQDs exhibited three energy band gaps at 3.35 eV, 3.92 eV, and 4.25 eV, suggesting multiple electronic transitions.

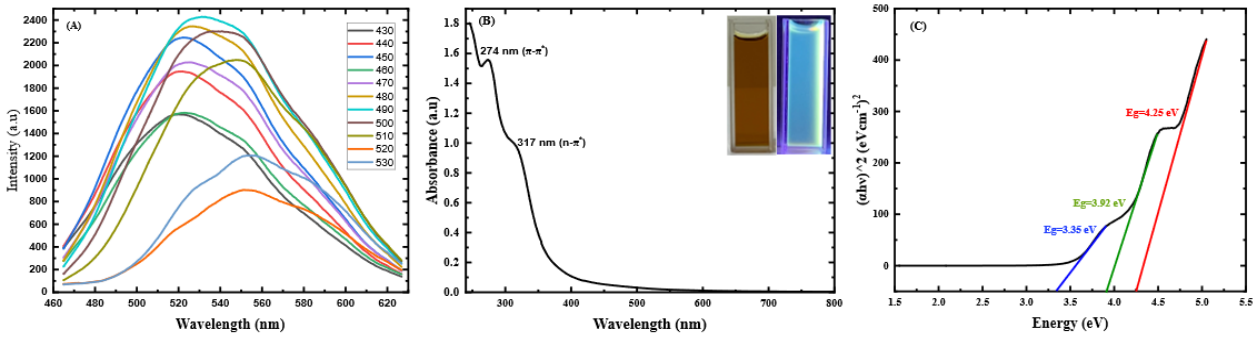

Figure 3: (A) Photoluminescence spectra of CQDs excited at various wavelengths; (B) Ultraviolet-visible absorption spectra of CQDs (with images of the CQD solution taken under natural light (left) and at 365 nm UV illumination (right), shown in the inset); (C) Tauc plot used to calculate the band gap energy of CQDs.

APPLICATIONS OF CQDs:

Detection of Cu^{2+} Ions:

To determine the CQDs' selectivity towards various metal ions, the fluorescence intensity of the CQDs was evaluated. The experiment was conducted in the presence of additional ions at an optimum wavelength of 490 nm, including (Ag^+, Fe^{3+}, Zn^{2+}, Cd^{2+}, Co^{2+}, Na^+, K^+, Hg^{2+}, Cu^{2+}, Cl^-, SO_4^{2-}, and NO_3^-). Figure 4A shows that introducing these ions into the CQD solutions had no noticeable effect on fluorescence intensity, except for copper (II) ions (Cu^{2+}), which specifically quenched the PL intensity. The findings indicate that the produced CQDs exhibit greater selectivity and sensitivity in detecting Cu^{2+} ions than other metal ions. Figure 4B shows images of the CQD solutions exposed to 365 nm UV light, revealing a significant reduction in the fluorescence intensity of CQDs following the addition of Cu^{2+} ions. The image on the left shows the CQD solution after adding Cu^{2+} ions, while the image on the right is the original CQD solution before adding Cu^{2+} ions.

By introducing different concentrations of Cu^{2+} ions into the CQD mixture, we investigated the response of the CQDs' fluorescence intensity for quantitative detection of Cu^{2+} ions. As seen in Figure 4C, the fluorescence intensity of the CQDs consistently decreased as the amounts of Cu^{2+} ion concentration increased. As Cu^{2+} ions of varying

quantities (ranging from 0.09 to 0.17 µM) were added, the fluorescence intensity diminished. With a correlation coefficient $R^2 = 0.975$, as demonstrated in Figure 4D, the observed changes demonstrate a strong linear association and are reversible. To investigate how Cu^{2+} ions affect the fluorescence characteristics of CQDs, the fluorescence intensity ratio to the quencher was measured using the Stern-Volmer equation (Zu *et al*., 2017). The fluorescence intensity ratio (I_0/I) of CQDs, where $I_0 = 2427$ arbitrary units (a.u.), represents the fluorescence intensity of produced CQDs at the optimum wavelength with no quencher, while I represents the fluorescence intensity of the CQDs in the presence of the quencher. The sensitivity of CQDs was estimated from the linear fit's slope by utilizing the coefficient of determination; the fitting yielded $R^2 = 0.987$, indicating that CQDs are an excellent sensor for Cu^{2+} ions with high precision, as illustrated in Figure 4E. The quenching impact demonstrates the robust and specific interaction between Cu^{2+} ions and CQDs.

The reduced limit of detection (LOD) of CQD fluorescence sensors renders them useful in numerous areas. A low level of detection indicates that the sensor exhibits high sensitivity. The limits of detection (LOD) and quantification (LOQ) were established utilizing the formulas provided by (Fu *et al*., 2017). The LOD for the synthesized CQDs is 0.1 micromolar (µM), while the limit of quantification is 0.3 µM. The standard deviation (σ) of the measurements used in the LOD and LOQ calculations was 50.1557 a.u./µM. Figure 4F demonstrates how the quencher affects the absorption characteristics of the CQDs. The absorption spectrum of CQDs shows a peak with an absorbance of 1.55 a.u. before introducing Cu^{2+} ions. Adding Cu^{2+} ions decreased the absorbance to 0.67 a.u., while the absorption peak wavelength remained unchanged. This suggests that Cu^{2+} ions interact with the CQDs through quenching mechanisms.

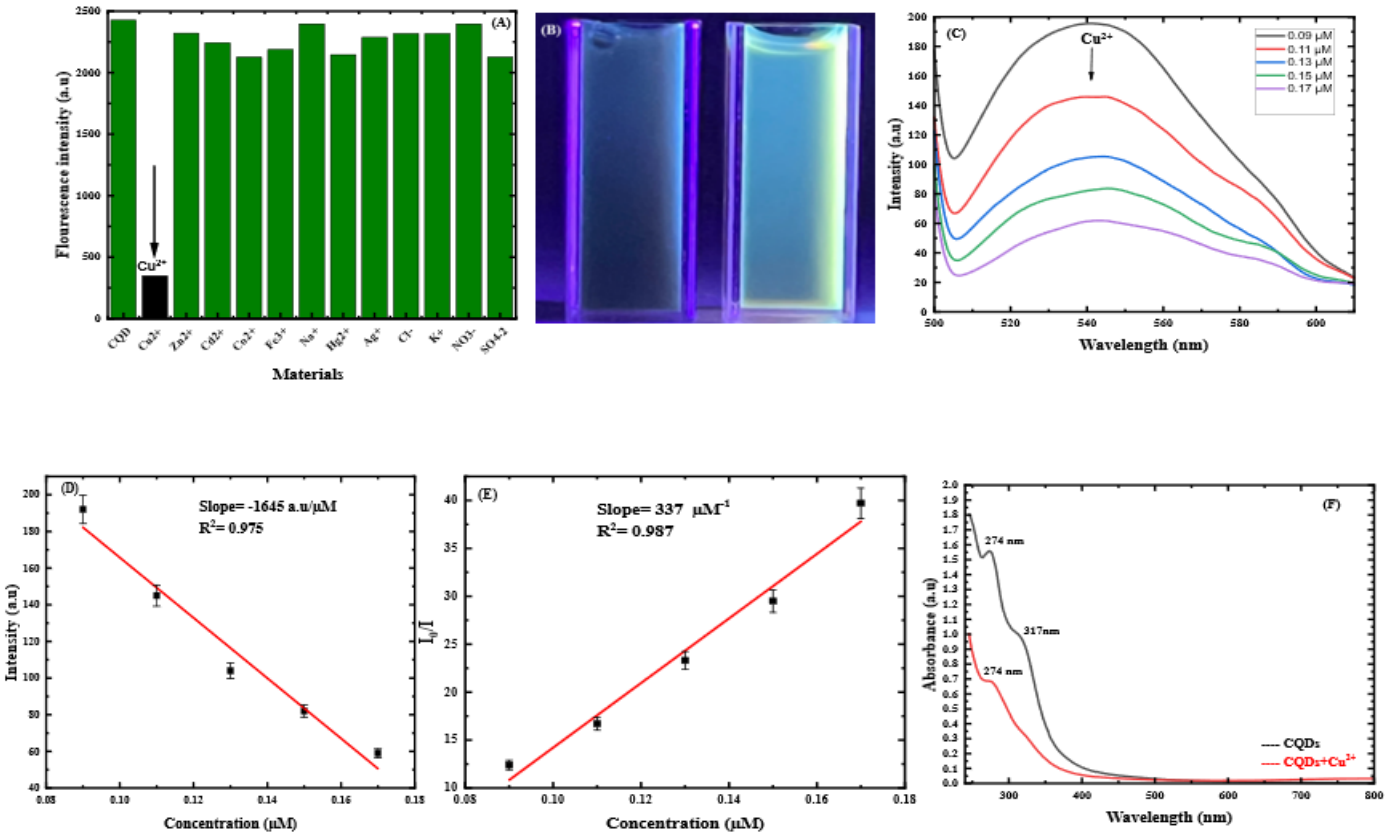

Figure 4: (A) Bar chart of the fluorescence intensity of CQDs when different materials are added, demonstrating their selectivity towards Cu^{2+} ions; (B) Images of CQD solutions under 365 nm UV illumination before (right) and after (left) adding Cu^{2+} ions; (C) Photoluminescence intensity changes of carbon quantum dots with varying concentrations of Cu^{2+} ions; (D) Correlation between fluorescence intensity of CQDs and Cu^{2+} ion concentrations; (E) Stern-Volmer plot showing the quenching mechanism and sensor response; (F) UV-Vis absorption spectra of synthesized CQDs in the absence and presence of Cu^{2+} ions.

CQD-Based Optical Nanothermometer:

The temperature-dependent fluorescence characteristics of the synthesized CQDs were studied to evaluate their potential effectiveness as optical nanothermometers. Figure 5A presents the CQDs' photoluminescence emission spectra, demonstrating their temperature dependence at an optimum excitation wavelength of 490 nm. As the temperature increased from 20 to 65 °C, in 5 °C increments, a gradual reduction in fluorescence intensity was observed at the emission peak of 537 nm. In contrast, the emission wavelength remained unchanged (Kalytchuk *et al*., 2017). As shown in Figure

5B, a strong correlation between the temperature and fluorescence intensity of CQDs was identified, featuring a coefficient of determination (R^2) of 0.9755. These findings indicate that the CQDs can function as precise nanothermometers within this range of temperatures, underscoring their potential for accurate thermal sensing and biological monitoring applications. The thermal sensitivity of the synthesized CQDs, as indicated by the slope of the linear fit (-9.198 a.u./°C), results in a relative thermal sensitivity (S_R) of 1.17% $°C^{-1}$ at 65°C (Sun *et al*., 2024).

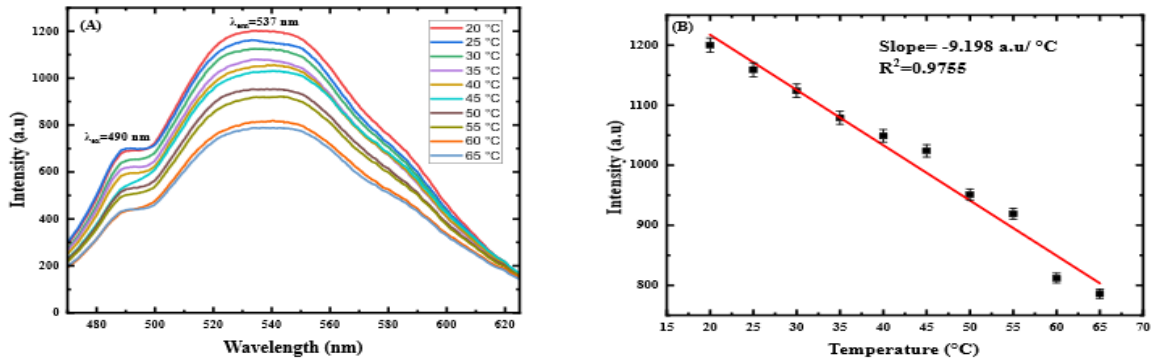

Figure 5: (A) Fluorescence emission spectra of CQDs over the temperature range of 20–65 °C; (B) Linear relationship between temperature and fluorescence intensity of the CQDs.

Antibacterial Activity of CQDs:

The produced CQDs' antibacterial effectiveness against Gram-negative bacteria, namely *Klebsiella and Escherichia coli (E. coli)*, was evaluated through the serial dilution method. Treatment with CQDs significantly reduced the number of *E. coli and Klebsiella* colonies, as shown in Figure 6. A consistent concentration of CQDs was applied to bacterial cultures that were diluted to 10^{-6}, 10^{-5}, and 10^{-4}. The culture plates provided visual evidence of the antibacterial effect. The findings indicated that *E. coli and Klebsiella* displayed decreased viability at all dilutions, demonstrating that CQDs inhibited bacterial growth and confirming their antibacterial properties of the CQDs regardless of bacterial density.

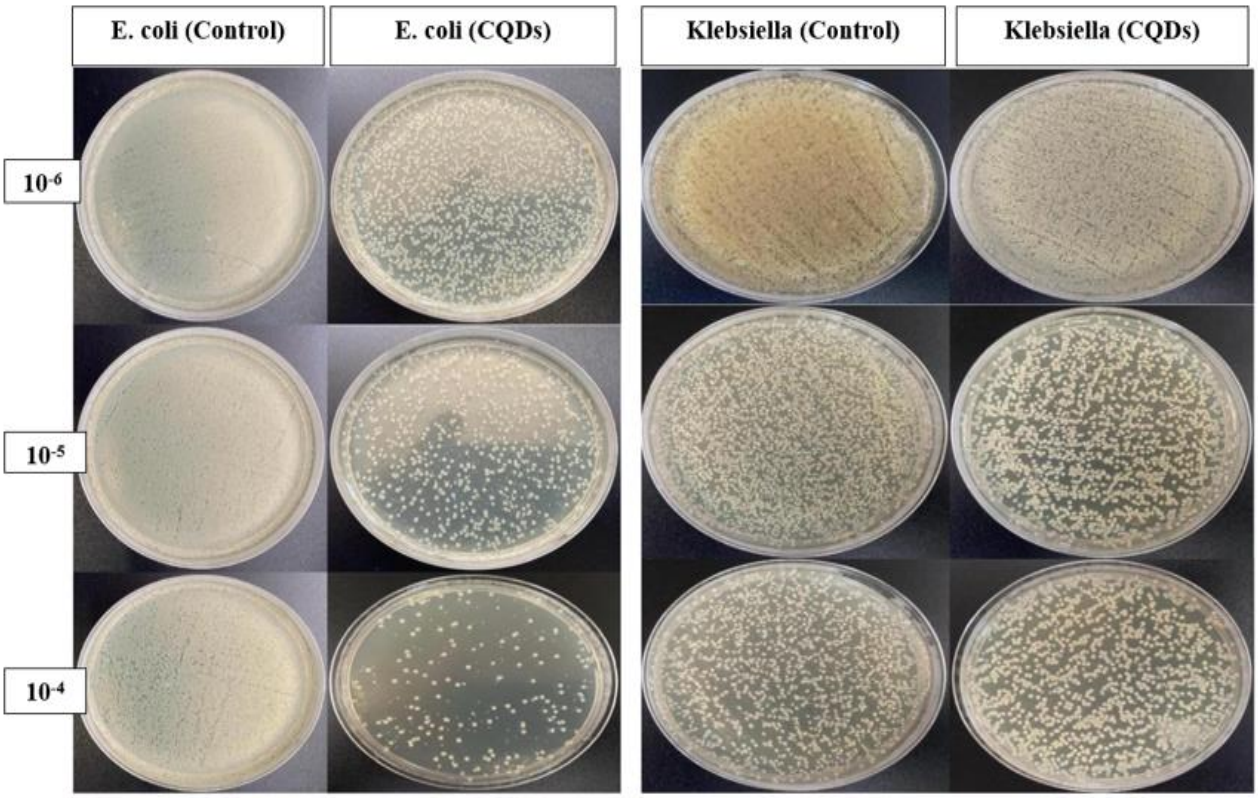

Figure 6: Photographic comparison of *E. coli* (left) and *Klebsiella* (right) colony formation under control (left) and CQD treatment (right) at various bacterial dilutions using the serial dilution method.

4. DISCUSSION

This study describes the green synthesis, characterization, and multi-applications of CQDs generated from green beans using a straightforward hydrothermal process. The prepared CQDs were found to be primarily quasi-spherical in shape and consisted of uniformly distributed nanoparticles with a small size distribution ranging from 2.35 nm to 9.82 nm, with an average particle size (d_{avg}) of 5.01 nm, which is in line with prior TEM results reported for CQDs made from citrus juice (Tadesse *et al*., 2018). The XRD analysis of the synthesized CQDs revealed that their reduced crystallinity and disordered structure were caused by the intrinsic growth of oxygen-containing functional groups. These results are supported by previous studies on the environmentally friendly production of CQDs using sugarcane industrial waste and Phyllanthus emblica fruit (Arul & Sethuraman, 2019; Pandiyan *et al*., 2020).

In addition, FTIR data show that oxygen functional groups (OH, C=O, and C-O-C) significantly enhance the water dispersibility and fluorescence efficiency of CQDs. This facilitates the creation of CQDs with notable surface functional groups aligning with sustainable, environmentally friendly methods (Sailaja Prasannakumaran Nair *et al*., 2020). Carbon quantum dots' elemental composition was studied by EDX spectroscopy. The produced CQDs are largely composed of oxygen and carbon atoms. The detection of oxygen indicates that oxygen-functional groups remain in the sample, while a high carbon percentage suggests that the precursor was successfully carbonized and converted into carbonaceous nanoparticles. Potassium appears to be present naturally in green bean seeds, as its detection occurred despite the absence of any external compounds containing potassium during synthesis. Surface-adsorbed potassium, partially integrated into CQD structures, can potentially affect the optical characteristics and surface charge of CQDs. Filtration and repeated washing with distilled water are two post-synthesis treatments that can effectively eliminate or reduce the most leftover potassium ions (Meiling *et al*., 2016).

Under 365 nm UV light, the produced carbon quantum dots fluoresced bright green and displayed excitation-dependent behavior in their photoluminescence emission spectra. Variations in particle size are the primary reason CQDs emit in response to different excitation wavelengths. Emission at specific wavelengths indicates variations in the band gaps of CQDs. In addition, this phenomenon is significantly influenced by the surface features of CQDs. The emission peaks can shift with the excitation wavelength when surface traps, functional groups, or defects create new energy states that affect the emission characteristics (Gan *et al*., 2016; Sharma *et al*., 2020). The CQDs prepared from green beans exhibited a fluorescence quantum yield of 37.1%. As demonstrated in Table 1, the obtained results exceeded those reported in the literature for hydrothermally synthesized CQDs from various eco-friendly sources. The oxygen-functional groups present in the green bean precursor improved surface passivation, thereby increasing fluorescence efficiency.

Table 1: Comparison of the fluorescence QYs of CQDs synthesized from natural precursors using the hydrothermal method.

Precursor	QY (%)	Ref.
Barberry	12.82	(Mohammadnejad & Ghiasi, 2025)
Red lentils	13.2	(Khan *et al*., 2019)
Chia seeds	17.8	(Marouzi *et al*., 2021)
Banana peel waste	20	(Atchudan *et al*., 2021)
Morus nigra fruit	24	(Atchudan *et al.*, 2022)
Sour whey	28	(Aydin *et al*., 2024)
Green bean seeds	37.1	This study

Two bands in the UV-Vis spectra indicate the formation of conjugated CQDs and the presence of surface groups containing oxygen (Sudolska *et al*., 2015). The CQDs exhibited three distinct energy band gaps at 3.35 eV, 3.92 eV, and 4.25 eV. The first energy gap at 3.35 eV can be attributed to surface-related defect states and localized electronic transitions associated with functional groups on the CQD surface. The second band gap at 3.92 eV corresponds to free electrons connected to oxygen atoms within sp^2 or sp^3 hybridized carbon structures. The highest energy band gap at 4.25 eV represents the π–π^* transition of sp^2 carbon domains in the CQDs (He *et al*., 2018; Kroupa *et al*., 2017). The presence of multiple band gaps is linked to the size heterogeneity of the CQDs, which leads to different degrees of quantum confinement, as well as the formation of various emissive states due to structural defects and surface functional groups. These findings are consistent with previous studies on biomass-derived CQDs, highlighting that both particle size variation and surface states significantly influence the optical properties of CQDs synthesized from green bean seeds (Elkun *et al*., 2024).

For practical applications, the synthesized CQDs serve as a cheap, safe, and effective method for detecting low concentrations of Cu^{2+} ions via fluorescence-based quenching mechanisms. Cu^{2+} ions interact with CQDs through electrostatic interactions between the ions and functional groups on the CQD surface. The pronounced linearity observed in the Stern-Volmer plot (Figure 4E) at low Cu^{2+} ion concentrations suggests that dynamic quenching is the predominant mechanism. Although a decrease in absorbance intensity from 1.55 to 0.67 without any wavelength shift was recorded upon the addition of Cu^{2+} ions, as shown in Figure 4F, this indicates potential weak interactions between the quencher and CQDs. Therefore, static quenching is likely present to a minor extent but does not play a significant role in this study (Liu *et al*., 2014; Luo *et al*., 2023). Table 2 summarizes

previously reported green carbon sources used to produce CQDs for Cu^{2+} ion detection. Their linear ranges and limits of detection vary depending on the precursor used. Green bean-derived CQDs demonstrated notable sensitivity, with a limit of detection (LOD) of 0.1µM, which is comparable to the other green precursors.

Table 2: Summary of green synthesized CQD-based sensors for Cu^{2+} ion detection.

Carbon source	LOD	Linear range	Ref.
Bamboo leaves	0.115 µM	0–66 µM	(Liu *et al*., 2014)
Prawn shell	5×10^{-3} µM	0.1–5 µM	(Gedda *et al*., 2016)
Sago waste	7.78 µM	0–47 µM	(Tan *et al*., 2014)
Kelp	7×10^{-3} µM	1–12.5 µM	(Zhu *et al*., 2017)
Grass	1×10^{-3} µM	0–50 µM	(Liu *et al*., 2012)
Green bean seeds	0.1 µM	0.09-0.17 µM	This study

Additionally, the synthesized CQDs demonstrated temperature-dependent fluorescence, exhibiting diminished intensity as the temperature rose from 20 to 65 °C. The reduction in fluorescence intensity with increasing temperature corresponds to the thermal activation of non-radiative trapping states. With increasing temperature, excited electrons are more likely to dissipate energy via thermal vibrations instead of photon emission, resulting in decreased quantum efficiency and, consequently, lower photoluminescence intensity (Zhao & Kim, 2017). The synthesized CQDs exhibited a relative temperature sensitivity of 1.17% $°C^{-1}$, markedly surpassing the sensitivities documented in certain prior investigations of carbon-based nanothermometers, as detailed in Table 3. The improved sensitivity underscores the capability of these CQDs as effective and precise fluorescent nanothermometers for real-time nanoscale temperature monitoring.

Table 3: Comparison of the temperature sensitivity of fluorescent CQDs synthesized from different carbon sources.

Carbon source	Linear range	Temperature sensitivity	Ref.
Citric acid	5-75 °C	0.41% $°C^{-1}$	(Zhang *et al*., 2019)
Trisodium citrate	10-70 °C	0.64% $°C^{-1}$	(Guo *et al*., 2020)
C_3N_4	20-80 °C	0.85% $°C^{-1}$	(Yang *et al*., 2015)
Green bean seeds	20-65 °C	1.17% $°C^{-1}$	This study

Furthermore, the present study provides visual evidence of antibacterial activity. Our findings show that CQDs exhibit a stronger inhibitory effect on *E. coli* compared to *Klebsiella* bacteria. The observed difference can be mainly assigned to the different features of their capsular structure and the mechanisms they employ for defense. *Klebsiella* features a thick polysaccharide capsule and strong antioxidative resistance mechanisms, which defend its outer membrane against CQDs. *Klebsiella* exhibited diminished responsiveness to CQD-induced membrane destabilization. In comparison, *E. coli* does not possess the comprehensive protective mechanisms and thick protective structures, rendering it more vulnerable to cellular damage (Zierke *et al*., 2025). This finding is consistent with previous studies that have shown carbon quantum dots derived from turmeric leaves to exhibit complete bactericidal activity against *E. coli* within an 8-hour period. In contrast, *Klebsiella* required 24 hours to achieve complete inhibition, attributed to the variation in their capsular structure (Saravanan *et al*., 2021). The ultrasmall size of the synthesized CQDs with a 5 nm diameter greatly enhances their antibacterial activity. The results confirm that CQDs are low-cost and environmentally-friendly antibacterial agents effective for bacteria-related infections. All the findings confirm that green bean-derived CQDs are cost-effective, sustainable, and multifunctional platforms that can be employed for environmental sensing, nanothermometry, and biomedical applications.

CONCLUSIONS AND RECOMMENDATIONS

This work reports a single-step hydrothermal technique for synthesizing green-bean-based multifunctional CQDs. The results of the characterization studies confirm the effective development of quasi-spherical CQDs with an average particle size of 5.01 nm and a surface capped with groups containing oxygen (–OH, C=O), greatly improving their excellent water dispersibility. The structural attributes support the photoluminescence (PL) analysis, which exhibits bright green fluorescence ($\lambda_{Ex}/\lambda_{Em}$ = 490/532 nm), leading to a notable quantum yield of 37.1%. The prepared CQDs demonstrate a selective fluorescence reduction in response to copper ions (Cu^{2+}) with an LOD of 0.1 µM. Additionally, the photoluminescence features of CQDs are explored through temperature sensitivity studies conducted in the range of 20-65 °C, highlighting their important application in nanoscale thermometry. The findings also reveal efficient antibacterial activity against *E. coli* and *Klebsiella* bacteria, with a stronger inhibitory effect observed against *E. coli*. Using low-cost and readily available biomass such as green beans represents a cost-effective and eco-friendly approach to synthesizing new nanomaterials with attractive features like small particle

size, rich functional groups, biocompatibility, intense green emission, excellent QY, and time-saving sensing properties. The findings demonstrate the remarkable versatility of green bean-derived CQDs in advanced fluorescence-based sensing and biomedical applications.

For the usability of CQDs to be increased, future studies need to explore new synthetic routes to produce CQDs with high stability and yields that emit longer-wavelength or near-infrared light. In addition, efforts must be made into expanding emission to longer wavelengths, e.g., yellow, orange, and red, beyond the typically reported blue and green regions. This development will greatly enhance the performance in a variety of potential uses, such as sensing, optoelectronics, and bioimaging. Furthermore, CQDs exhibit significant potential as core materials for the next phase in nanocomposite materials due to their multifunctional characteristic, affordability, safety, and improved biocompatibility. Following the principles of green chemistry, developing CQD-based nanocomposites from waste- or biomass-derived precursors using low-energy and environmentally friendly pathways can induce a tremendous research renaissance in material science applications.

Acknowledgement:

I wish to express my sincere thanks to the Physics Research Center, University of Zakho, for providing the essential facilities and support throughout this research journey.

Author Contributions:

All authors contributed equally to the conception, implementation, review, and writing of this manuscript.

Ethical Approval:

In this research, no experiments involving humans or animals were conducted, and no institutional support was sought; therefore, ethical approval was not required.

REFERENCES

Arul, V., & Sethuraman, M. G. (2019). Hydrothermally green synthesized nitrogen-doped carbon dots from Phyllanthus emblica and their catalytic ability in the detoxification of textile effluents. *ACS omega*, *4*(2), 3449-3457. https://doi.org/10.1021/acsomega.8b03674

Atchudan, R., Edison, T. N. J. I., Perumal, S., Vinodh, R., Sundramoorthy, A. K., Babu, R. S., & Lee, Y. R. (2022). Morus nigra-derived hydrophilic carbon dots for the highly selective and sensitive detection of ferric ion in aqueous media and human colon cancer cell imaging. *Colloids and Surfaces A: Physicochemical and Engineering Aspects*, *635*, 128073. https://doi.org/10.1016/j.colsurfa.2021.128073

Atchudan, R., Edison, T. N. J. I., Shanmugam, M., Perumal, S., Somanathan, T., & Lee, Y. R. (2021). Sustainable synthesis of carbon quantum dots from banana peel waste using hydrothermal process for in vivo bioimaging. *Physica E: Low-dimensional Systems and Nanostructures*, *126*, 114417. https://doi.org/10.1016/j.physe.2020.114417

Aydin, S., Yilmaz, A., & Yilmaz, M. (2024). Green Synthesis of Various Heteroatom-doped Carbon Quantum Dots from Urine, Whey, and Their Mixture: The Optimization of Synthesis and Potential Applications. *ChemistrySelect*, *9*(17), e202304930. https://doi.org/10.1002/slct.202304930

Bakier, Y., Ghali, M., & Zahra, W. (2020). Highly sensitive fluorescent detection of pyridine using small size carbon quantum dots derived from folic acid. *Journal of Physics D: Applied Physics*, *53*(40), 405103. https://doi.org/10.1088/1361-6463/ab985e

Bandi, R., Gangapuram, B. R., Dadigala, R., Eslavath, R., Singh, S. S., & Guttena, V. (2016). Facile and green synthesis of fluorescent carbon dots from onion waste and their potential applications as sensor and multicolour imaging agents. *Rsc Advances*, *6*(34), 28633-28639. https://doi.org/10.1039/C6RA01669C

Bucka, K., Socha, R. P., & Wojnicki, M. (2024). Carbon Quantum Dots as Phosphors in LEDs: Perspectives and Limitations—A Critical Review of the Literature. *Electronics*, *13*(22), 4481. https://doi.org/10.3390/electronics13224481

Chahal, S., Macairan, J.-R., Yousefi, N., Tufenkji, N., & Naccache, R. (2021). Green synthesis of carbon dots and their applications. *Rsc Advances*, *11*(41), 25354-25363. https://doi.org/10.1039/D1RA04718C

D'Souza, L. F., Jadhav, R. W., Bhosale, S. V., & Bugde, S. T. (2024). Crafting carbon quantum dots from acetone: dual purpose Fe3+ ion and pH sensing platform. *Emergent Materials*, 1-12. https://doi.org/10.1007/s42247-024-00792-0

Das, P., Maruthapandi, M., Saravanan, A., Natan, M., Jacobi, G., Banin, E., & Gedanken, A. (2020). Carbon dots for heavy-metal sensing, pH-sensitive cargo delivery, and antibacterial applications. *ACS Applied Nano Materials*, *3*(12), 11777-11790. https://doi.org/10.1021/acsanm.0c02305

Das, S., Mondal, S., & Ghosh, D. (2024). Carbon quantum dots in bioimaging and biomedicines. *Frontiers in bioengineering and biotechnology*, *11*, 1333752. https://doi.org/10.3389/fbioe.2023.1333752

Deme, G., Belay, A., Andoshe, D. M., Barsisa, G., Tsegaye, D., Tiruneh, S., & Seboka, C. (2023). Effect of hydrothermal reaction temperature on fluorescent properties of carbon quantum dots synthesized from lemon juice for adsorption applications. *Journal of Nanomaterials*, *2023*(1), 1701496. https://doi.org/10.1155/2023/1701496

Elkun, S., Ghali, M., Sharshar, T., & Mosaad, M. M. (2024). Green synthesis of fluorescent N-doped carbon quantum dots from castor seeds and their applications in cell imaging and pH sensing. *Scientific Reports*, *14*(1), 27927. https://doi.org/10.1038/s41598-024-78745-0

Feng, Y., Zhong, D., Miao, H., & Yang, X. (2015). Carbon dots derived from rose flowers for tetracycline sensing. *Talanta*, *140*, 128-133. https://doi.org/10.1016/j.talanta.2015.03.038

Fu, H., Ji, Z., Chen, X., Cheng, A., Liu, S., Gong, P., Li, G., Chen, G., Sun, Z., & Zhao, X. (2017). A

versatile ratiometric nanosensing approach for sensitive and accurate detection of Hg 2+ and biological thiols based on new fluorescent carbon quantum dots. *Analytical and bioanalytical chemistry*, *409*, 2373-2382. https://doi.org/10.1007/s00216-017-0183-3

Gagic, M., Kociova, S., Smerkova, K., Michalkova, H., Setka, M., Svec, P., Pribyl, J., Masilko, J., Balkova, R., & Heger, Z. (2020). One-pot synthesis of natural amine-modified biocompatible carbon quantum dots with antibacterial activity. *Journal of Colloid and Interface Science*, *580*, 30-48. https://doi.org/10.1016/j.jcis.2020.06.125

Gan, Z., Xu, H., & Hao, Y. (2016). Mechanism for excitation-dependent photoluminescence from graphene quantum dots and other graphene oxide derivates: consensus, debates and challenges. *Nanoscale*, *8*(15), 7794-7807. https://doi.org/10.1039/C6NR00605A

Gedda, G., Lee, C.-Y., Lin, Y.-C., & Wu, H.-f. (2016). Green synthesis of carbon dots from prawn shells for highly selective and sensitive detection of copper ions. *Sensors and Actuators B: Chemical*, *224*, 396-403. https://doi.org/10.1016/j.snb.2015.09.065

Guo, Z., Luo, J., Zhu, Z., Sun, Z., Zhang, X., Wu, Z.-c., Mo, F., & Guan, A. (2020). A facile synthesis of high-efficient N, S co-doped carbon dots for temperature sensing application. *Dyes and Pigments*, *173*, 107952. https://doi.org/10.1016/j.dyepig.2019.107952

He, S., Turnbull, M. J., Nie, Y., Sun, X., & Ding, Z. (2018). Band structures of blue luminescent nitrogen-doped graphene quantum dots by synchrotron-based XPS. *Surface Science*, *676*, 51-55. https://doi.org/10.1016/j.susc.2018.01.013

Hu, M., Guo, D., Tang, J., Liu, K., Lian, H., Xu, C., Xu, L., & Zhang, W. (2022). Temperature sensing performance of fluorescent carbon quantum dots prepared from loblolly pine processing waste. *Russian Journal of Physical Chemistry A*, *96*(14), 3070-3081. https://doi.org/10.1134/S0036024423030202

Hu, S., Trinchi, A., Atkin, P., & Cole, I. (2015). Tunable photoluminescence across the entire visible spectrum from carbon dots excited by white light. *Angewandte Chemie International Edition*, *54*(10), 2970-2974. https://doi.org/10.1002/anie.201411004

Jia, J., Lin, B., Gao, Y., Jiao, Y., Li, L., Dong, C., & Shuang, S. (2019). Highly luminescent N-doped carbon dots from black soya beans for free radical scavenging, Fe3+ sensing and cellular imaging. *Spectrochimica Acta Part A: Molecular and Biomolecular Spectroscopy*, *211*, 363-372. https://doi.org/10.1016/j.saa.2018.12.034

Jumardin, J., Maddu, A., Santoso, K., & Isnaeni, I. (2021). Synthesis of carbon dots (CDS) and determination of optical gap energy with Tauc plot method. *Jambura Physics Journal*, *3*(2), 73-86. https://doi.org/10.34312/jpj.v3i2.11235

Kalytchuk, S., Poláková, K. i., Wang, Y., Froning, J. P., Cepe, K., Rogach, A. L., & Zbořil, R. (2017). Carbon dot nanothermometry: intracellular photoluminescence lifetime thermal sensing. *ACS nano*, *11*(2), 1432-1442. https://doi.org/10.1021/acsnano.6b06670

Kaur, N., Sharma, V., Tiwari, P., Saini, A. K., & Mobin, S. M. (2019). "Vigna radiata" based green C-dots: photo-triggered theranostics, fluorescent sensor for extracellular and intracellular iron (III) and multicolor live cell imaging probe. *Sensors and Actuators B: Chemical*, *291*, 275-286. https://doi.org/10.1016/j.snb.2019.04.039

Khan, Z. M., Rahman, R. S., Islam, S., & Zulfequar, M. (2019). Hydrothermal treatment of red lentils for the synthesis of fluorescent carbon quantum dots and its application for sensing Fe3+. *Optical Materials*, *91*, 386-395. https://doi.org/10.1016/j.optmat.2019.03.054

Kong, J., Wei, Y., Zhou, F., Shi, L., Zhao, S., Wan, M., & Zhang, X. (2024). Carbon quantum dots: properties, preparation, and applications. *Molecules*, *29*(9), 2002. https://doi.org/10.3390/molecules29092002

Kroupa, D. M., Vörös, M., Brawand, N. P., McNichols, B. W., Miller, E. M., Gu, J., Nozik, A. J., Sellinger, A., Galli, G., & Beard, M. C. (2017). Tuning colloidal quantum dot band edge positions through solution-phase surface chemistry modification. *Nature Communications*, *8*(1), 15257. https://doi.org/10.1038/ncomms15257

Kumar, S., Goswami, M., Singh, N., Sathish, N., Reddy, M., & Kumar, S. (2022). Exploring carbon quantum dots as an aqueous electrolyte for energy storage devices. *Journal of Energy Storage*, *55*, 105522. https://doi.org/10.1016/j.est.2022.105522

Li, T., Li, Z., Huang, T., & Tian, L. (2021). Carbon quantum dot-based sensors for food safety. *Sensors and Actuators A: Physical*, *331*, 113003. https://doi.org/10.1016/j.sna.2021.113003

Liu, S., Tian, J., Wang, L., Zhang, Y., Qin, X., Luo, Y., Asiri, A. M., Al-Youbi, A. O., & Sun, X. (2012). Hydrothermal treatment of grass: a low-cost, green route to nitrogen-doped, carbon-rich, photoluminescent polymer nanodots as an effective fluorescent sensing platform for label-free detection of Cu (II) ions. *Advanced materials*, *24*(15), 2037. https://doi.org/10.1002/adma.201200164

Liu, Y., Zhao, Y., & Zhang, Y. (2014). One-step green synthesized fluorescent carbon nanodots from bamboo leaves for copper (II) ion detection. *Sensors and Actuators B: Chemical*, *196*, 647-652.

Luo, Y., Cui, C., Zhang, X., Jiang, Y., Xiang, Z., Ji, C., & Peng, Z. (2023). Carbon dots-based fluorescence assay for the facile and reliable detection of Ag+ in natural water and serum samples. *Molecules*, *28*(4), 1566. https://doi.org/10.3390/molecules28041566

Magesh, V., Sundramoorthy, A. K., & Ganapathy, D. (2022). Recent advances on synthesis and potential applications of carbon quantum dots. *Frontiers in materials*, *9*, 906838. https://doi.org/10.3389/fmats.2022.906838

Marouzi, S., Darroudi, M., Hekmat, A., Sadri, K., & Oskuee, R. K. (2021). One-pot hydrothermal

synthesis of carbon quantum dots from Salvia hispanica L. seeds and investigation of their biodistribution, and cytotoxicity effects. *Journal of Environmental Chemical Engineering*, *9*(4), 105461. https://doi.org/10.1016/j.jece.2021.105461

Mehta, V. N., Jha, S., Basu, H., Singhal, R. K., & Kailasa, S. K. (2015). One-step hydrothermal approach to fabricate carbon dots from apple juice for imaging of mycobacterium and fungal cells. *Sensors and Actuators B: Chemical*, *213*, 434-443. https://doi.org/10.1016/j.snb.2015.02.104

Meiling, T. T., Cywiński, P. J., & Bald, I. (2016). White carbon: Fluorescent carbon nanoparticles with tunable quantum yield in a reproducible green synthesis. *Scientific Reports*, *6*(1), 28557. https://doi.org/10.1038/srep28557

Mohammadnejad, M., & Ghiasi, M. (2025). Green synthesis of a fluorescence optical probe for Fe3+ based on Barberry derived carbon quantum dots: Deep insight on interaction from experimental and theoretical approach. *Spectrochimica Acta Part A: Molecular and Biomolecular Spectroscopy*, 125775. https://doi.org/10.1016/j.saa.2025.125775

Mohammed, L. J., & Omer, K. M. (2020). Dual functional highly luminescence B, N Co-doped carbon nanodots as nanothermometer and Fe3+/Fe2+ sensor. *Scientific Reports*, *10*(1), 3028. https://doi.org/10.1038/s41598-020-59958-5

Molaei, M. J. (2023). Carbon quantum dots-based fluorescent layered double hydroxide for targeted drug delivery application. *Diamond and Related Materials*, *137*, 110135. https://doi.org/10.1016/j.diamond.2023.110135

Mousa, M. A., Abdelrahman, H. H., Fahmy, M. A., Ebrahim, D. G., & Moustafa, A. H. (2023). Pure and doped carbon quantum dots as fluorescent probes for the detection of phenol compounds and antibiotics in aquariums. *Scientific Reports*, *13*(1), 12863. https://doi.org/10.1038/s41598-023-39490-y

Nazibudin, N. A., Zainuddin, M. F., & Abdullah, C. A. C. (2023). Hydrothermal synthesis of carbon quantum dots: An updated review. *J. Adv. Res. Fluid Mech. Therm. Sci*, *101*, 192-206. https://doi.org/10.37934/arfmts.101.1.192206

Pandiyan, S., Arumugam, L., Srirengan, S. P., Pitchan, R., Sevugan, P., Kannan, K., Pitchan, G., Hegde, T. A., & Gandhirajan, V. (2020). Biocompatible carbon quantum dots derived from sugarcane industrial wastes for effective nonlinear optical behavior and antimicrobial activity applications. *ACS omega*, *5*(47), 30363-30372. https://doi.org/10.1021/acsomega.0c03290

Saber, Y. A., Hamed, M., Emara, S., Mansour, F. R., Locatelli, M., & Ibrahim, N. (2024). Garlic peel-based carbon quantum dots as a sustainable alternative for the sensitive and green spectrofluorometric quantification of molnupiravir in pharmaceutical capsules. *Heliyon*, *10*(23). https://doi.org/10.1016/j.heliyon.2024.e40661

Sailaja Prasannakumaran Nair, S., Kottam, N., & SG, P. K. (2020). Green synthesized luminescent carbon nanodots for the sensing application of Fe3+ ions. *Journal of Fluorescence*, *30*(2), 357-363. https://doi.org/10.1007/s10895-020-02505-2

Salman, B. I. (2023). A novel design eco-friendly microwave-assisted Cu–N@ CQDs sensor for the quantification of eravacycline via spectrofluorimetric method; application to greenness assessments, dosage form and biological samples. *Journal of Fluorescence*, *33*(5), 1887-1896. https://doi.org/10.1007/s10895-023-03190-7

Saravanan, A., Maruthapandi, M., Das, P., Luong, J. H., & Gedanken, A. (2021). Green synthesis of multifunctional carbon dots with antibacterial activities. *Nanomaterials*, *11*(2), 369. https://doi.org/10.3390/nano11020369

Scaria, J., Karim, A. V., Divyapriya, G., Nidheesh, P., & Kumar, M. S. (2020). Carbon-supported semiconductor nanoparticles as effective photocatalysts for water and wastewater treatment. In *Nano-Materials as Photocatalysts for Degradation of Environmental Pollutants* (pp. 245-278). Elsevier. https://doi.org/10.1016/B978-0-12-818598-8.00013-4

Sciortino, A., Cannizzo, A., & Messina, F. (2018). Carbon nanodots: a review—from the current understanding of the fundamental photophysics to the full control of the optical response. *C*, *4*(4), 67. https://doi.org/10.3390/c4040067

Sharma, N., Das, G. S., & Yun, K. (2020). Green synthesis of multipurpose carbon quantum dots from red cabbage and estimation of their antioxidant potential and bio-labeling activity. *Applied Microbiology and Biotechnology*, *104*, 7187-7200. https://doi.org/10.1007/s00253-020-10726-5

Singh, M., Manickavasagan, A., Shobana, S., & Mohan, V. (2021). Glycemic index of pulses and pulse-based products: a review. *Critical Reviews in Food Science and Nutrition*, *61*(9), 1567-1588. https://doi.org/10.1080/10408398.2020.1762162

Sudolska, M., Dubecky, M., Sarkar, S., Reckmeier, C. J., Zboril, R., Rogach, A. L., & Otyepka, M. (2015). Nature of absorption bands in oxygen-functionalized graphitic carbon dots. *The Journal of Physical Chemistry C*, *119*(23), 13369-13373. https://doi.org/10.1021/acs.jpcc.5b04080

Sun, J., Yan, K., Zhang, P., Pan, A., Chen, X., & Shi, X. (2024). Green-emitting carbon quantum dots: highly sensitive temperature sensing probe in nanocomposite and lubrication system. *Lubricants*, *12*(3), 88. https://doi.org/10.3390/lubricants12030088

Tadesse, A., RamaDevi, D., Hagos, M., Battu, G., & Basavaiah, K. (2018). Facile green synthesis of fluorescent carbon quantum dots from citrus lemon juice for live cell imaging. *Asian J. Nanosci. Mater*, *1*(1), 36-46. https://doi.org/10.26655/ajn-anom-at.2018.1.5

Tan, X. W., Romainor, A. N. B., Chin, S. F., & Ng, S. M. (2014). Carbon dots production via pyrolysis of sago waste as potential probe for metal ions sensing. *Journal of analytical and applied pyrolysis*, *105*, 157-165. https://doi.org/10.1016/j.jaap.2013.11.001

Verma, S. K., Das, A. K., Gantait, S., Panwar, Y., Kumar, V., & Brestic, M. (2022). Green synthesis of carbon-based nanomaterials and their applications in various sectors: a topical review. *Carbon Letters*, *32*(2), 365-393. https://doi.org/10.1007/s42823-021-00294-7

Xie, Y., Zheng, J., Wang, Y., Wang, J., Yang, Y., Liu, X., & Chen, Y. (2019). One-step hydrothermal synthesis of fluorescence carbon quantum dots with high product yield and quantum yield. *Nanotechnology*, *30*(8), 085406. https://doi.org/10.1088/1361-6528/aaf3fb

Xu, Q., Gao, J., Wang, S., Wang, Y., Liu, D., & Wang, J. (2021). Quantum dots in cell imaging and their safety issues. *Journal of Materials Chemistry B*, *9*(29), 5765-5779. https://doi.org/10.1039/D1TB00729G

Yadav, P. K., Chandra, S., Kumar, V., Kumar, D., & Hasan, S. H. (2023). Carbon quantum dots: synthesis, structure, properties, and catalytic applications for organic synthesis. *Catalysts*, *13*(2), 422. https://doi.org/10.3390/catal13020422

Yang, Y., Kong, W., Li, H., Liu, J., Yang, M., Huang, H., Liu, Y., Wang, Z., Wang, Z., & Sham, T.-K. (2015). Fluorescent N-doped carbon dots as in vitro and in vivo nanothermometer. *ACS Applied Materials & Interfaces*, *7*(49), 27324-27330. https://doi.org/10.1021/acsami.5b08782

Yin, B., Deng, J., Peng, X., Long, Q., Zhao, J., Lu, Q., Chen, Q., Li, H., Tang, H., & Zhang, Y. (2013). Green synthesis of carbon dots with down-and up-conversion fluorescent properties for sensitive detection of hypochlorite with a dual-readout assay. *Analyst*, *138*(21), 6551-6557. https://doi.org/10.1039/C3AN01003A

Yuan, T., Meng, T., He, P., Shi, Y., Li, Y., Li, X., Fan, L., & Yang, S. (2019). Carbon quantum dots: an emerging material for optoelectronic applications. *Journal of Materials Chemistry C*, *7*(23), 6820-6835. https://doi.org/10.1039/C9TC01730E

Zhang, J., Nan, D., Pan, S., Liu, H., Yang, H., & Hu, X. (2019). N, S co-doped carbon dots as a dual-functional fluorescent sensor for sensitive detection of baicalein and temperature. *Spectrochimica Acta Part A: Molecular and Biomolecular Spectroscopy*, *221*, 117161. https://doi.org/10.1016/j.saa.2019.117161

Zhang, Z., Sun, W., & Wu, P. (2015). Highly photoluminescent carbon dots derived from egg white: facile and green synthesis, photoluminescence properties, and multiple applications. *ACS Sustainable Chemistry & Engineering*, *3*(7), 1412-1418. https://doi.org/10.1021/acssuschemeng.5b00156

Zhao, F., & Kim, J. (2017). The effect of temperature on photoluminescence enhancement of quantum dots in brain slices. *Journal of Nanoscience and Nanotechnology*, *17*(4), 2606-2609. https://doi.org/10.1166/jnn.2017.13332

Zhu, X., Jin, H., Gao, C., Gui, R., & Wang, Z. (2017). Ratiometric, visual, dual-signal fluorescent sensing and imaging of pH/copper ions in real samples based on carbon dots-fluorescein isothiocyanate composites. *Talanta*, *162*, 65-71. https://doi.org/10.1016/j.talanta.2016.10.015

Zierke, L., Mourad, R., Kohler, T. P., Müsken, M., & Hammerschmidt, S. (2025). Influence of the polysaccharide capsule on virulence and fitness of Klebsiella pneumoniae. *Frontiers in microbiology*, *16*, 1450984. https://doi.org/10.3389/fmicb.2025.1450984

Zu, F., Yan, F., Bai, Z., Xu, J., Wang, Y., Huang, Y., & Zhou, X. (2017). The quenching of the fluorescence of carbon dots: a review on mechanisms and applications. *Microchimica Acta*, *184*, 1899-1914. https://doi.org/10.1007/s00604-017-2318-9

Zulfajri, M., Abdelhamid, H. N., Sudewi, S., Dayalan, S., Rasool, A., Habib, A., & Huang, G. G. (2020). Plant part-derived carbon dots for biosensing. *Biosensors*, *10*(6), 68. https://doi.org/10.3390/bios10060068